

# Densification and grain growth in BaTiO<sub>3</sub> ceramics fabricated from nanopowders synthesized by ball-milling assisted hydrothermal reaction

Yuji Hotta<sup>a,\*</sup>, Cihangir Duran<sup>a,b</sup>, Kimiyasu Sato<sup>a</sup>, Takaaki Nagaoka<sup>a</sup>, Koji Watari<sup>a</sup>

<sup>a</sup> National Institute of Advanced Industrial Science and Technology (AIST), Anagahora 2266-98, Shimoshidami, Moriyama-ku, Nagoya 463-8560, Japan

<sup>b</sup> Gebze Institute of Technology, Department of Materials Science and Engineering, PK 141, 41400 Gebze, Kocaeli, Turkey

Received 16 May 2007; received in revised form 10 July 2007; accepted 14 July 2007

Available online 12 September 2007

## Abstract

BaTiO<sub>3</sub> powders synthesized by hydrothermal reaction assisted with or without ball milling were used to fabricate sintered bulk BaTiO<sub>3</sub> ceramics. The sintering rate of BaTiO<sub>3</sub> green compacts produced by ball-milling assisted hydrothermal reaction was found to be faster than that prepared by hydrothermal reaction without ball milling. In the case of green compacts produced by BaTiO<sub>3</sub> powders synthesized without ball milling, the relative density and the shrinkage of sintered compacts were measured to be 60% and 5% at 900 °C and 94.3% and 13% at 1000 °C, respectively. On the other hand, the relative density and the shrinkage of sintered compacts produced by ball-milling assisted hydrothermal reaction were measured to be 96.5% and 8% at 900 °C and 98.6% and 24% at 1000 °C, respectively. Furthermore, the free energy for grain-growth activation was estimated from the relationship between grain size and sintering temperature. The free energy for grain-growth activation of the sample produced by the hydrothermal reaction assisted with or without ball milling was calculated to be  $4.2 \times 10^5$  and  $8.4 \times 10^5$  J/mol, respectively. It was found that the grain-growth of green compacts produced by assistance of ball milling was promoted at lower-sintering temperature.

© 2007 Elsevier Ltd. All rights reserved.

**Keywords:** Hydrothermal reaction; Milling; Sintering; Grain growth; BaTiO<sub>3</sub>

## 1. Introduction

Hydrothermal method has the advantages of synthesizing high-purity and single-phase oxides at a relatively faster rate under solvent vapor pressure. The moderate temperature required in this method not only enhances the reactivity of the products but also reduces the energy cost. Furthermore, a variety of particle morphologies can be produced.<sup>1</sup>

Barium titanate (BaTiO<sub>3</sub>) is a well-known dielectric material with high permittivity and one of the most widely used materials in electronic ceramics. It has been utilized especially for multi-layer ceramic capacitors (MLCCs) because of its high dielectric characteristics.<sup>2</sup> The conventional method of synthesizing BaTiO<sub>3</sub> powder is the solid-state reaction between barium carbonate (BaCO<sub>3</sub>) and titania (TiO<sub>2</sub>) above 1100 °C. Therefore, the sintered compacts are produced above 1300 °C. Furthermore, BaTiO<sub>3</sub> prepared from the solid-state reaction exhibits some drawbacks, such as a large particle size, wide

particle size distribution, aggregation and high impurity contents, which results from repetitive calcination and grinding treatments.<sup>3</sup> Recently, wet chemical technologies such as the sol-gel method<sup>4,5</sup> and hydrothermal method<sup>6–12</sup> have replaced the classical solid-state reaction for the synthesis of BaTiO<sub>3</sub> powders. Solution chemistry and alkoxides precursors allow a much smaller mixing range between barium and titanium ions. Hence, wet chemical technologies have led to homogeneous, phase-pure BaTiO<sub>3</sub> with finer particle size, and, therefore, BaTiO<sub>3</sub> ceramics are expected to be fabricated at much lower-sintering temperatures. In fact, nano-sized BaTiO<sub>3</sub> powders have been synthesized by hydrothermal method.<sup>13,14</sup> However, it is difficult to prepare dense BaTiO<sub>3</sub> bulk ceramics using nano-sized powder via a conventional sintering process because nano-sized particles have tendency to form agglomerates. Therefore, the sintering temperature of green compacts consisted of nano-sized particles is not lower.

Ball milling techniques are widely used for grinding of agglomerated powders and preparation of a dispersed suspension.<sup>15,16</sup> If ball media is introduced during the hydrothermal reaction, this technique is expected to promote the reaction of barium and titanium ions and to change the surface properties

\* Corresponding author. Tel.: +81 52 736 7383; fax: +81 52 736 7405.  
E-mail address: [y-hotta@aist.go.jp](mailto:y-hotta@aist.go.jp) (Y. Hotta).

of  $\text{BaTiO}_3$  powders formed. Recently, synthesis of  $\beta\text{-LiFe}_5\text{O}_8$  particles by the hydrothermal planetary ball milling was reported, indicating that the fine  $\beta\text{-LiFe}_5\text{O}_8$  particles could be prepared by milling during the hydrothermal reaction.<sup>17</sup> Furthermore, we reported that  $\text{BaTiO}_3$  powders prepared from ball-milling assisted hydrothermal reaction could sinter at fairly low temperatures.

In this work, densification and grain growth in  $\text{BaTiO}_3$  ceramics fabricated from powders synthesized by ball-milling assisted hydrothermal reaction is reported and compared with those prepared without ball milling. Free energy for grain-growth in  $\text{BaTiO}_3$  ceramics will also be discussed in regard to ball milling effect during hydrothermal reaction.

## 2. Experimental procedure

### 2.1. Preparation of $\text{BaTiO}_3$ nanopowders and green compacts

The  $\text{BaTiO}_3$  powders were synthesized by using  $\text{Ba}(\text{OH})_2 \cdot 8\text{H}_2\text{O}$  (Wako Pure Chemical Industries, Japan) and titanium tetraisopropoxide ( $\text{Ti}(\text{i-OPr})_4$ , TTIP, Wako, Japan). The high pH necessary for the reaction was provided by introducing an excess of  $\text{Ba}(\text{OH})_2 \cdot 8\text{H}_2\text{O}$ .<sup>8</sup> All chemicals were used as received without further purification.  $\text{Ba}(\text{OH})_2 \cdot 8\text{H}_2\text{O}$  was dissolved in hot water at  $80^\circ\text{C}$  and quickly filtered to remove  $\text{BaCO}_3$ . After TTIP was diluted in isopropyl alcohol, the solution was dropped into the  $\text{Ba}(\text{OH})_2$  solution under vigorous stirring. The mole ratio of Ba to Ti before the removal of  $\text{BaCO}_3$  was adjusted to 1.5:1. In this work,  $\text{BaTiO}_3$  powders were prepared by a novel hydrothermal synthesis apparatus with ball milling system developed for this study (Fig. 1). The hydrothermal treatments assisted with or without ball milling

were performed at  $100^\circ\text{C}$  for 2 h, as shown in Fig. 1. The mixed starting solution was transferred to a Teflon vessel and 5 mm  $\text{ZrO}_2$  balls were added. Then, the sealed Teflon vessel was put into a stainless-steel vessel. Heating and cooling rates were performed at  $200^\circ\text{C}/\text{h}$ . The synthesis temperature was maintained at  $100^\circ\text{C}$  for 2 h, under autogenous water vapor pressure and the vessel was rotated at 150 rpm during the hydrothermal reaction. After the reaction, the suspension was centrifuged and the resulting solid was washed several times in water to remove unreacted Ba ions. The solid was finally freeze-dried. Green bodies were fabricated by first uniaxial dry pressing at 20 MPa in a steel die and then cold isostatic pressing (CIP) at 150 MPa for 5 min. The relative densities of the green bodies prepared by hydrothermal reaction with/without ball milling system were calculated to be 52% and 53%. The green bodies were sintered at various temperatures for 5 h. For the sake of comparison, green bodies using powders synthesized by hydrothermal reaction without ball milling were also prepared. The synthesis of  $\text{BaTiO}_3$  powders was reported in detail in our earlier study.

### 2.2. Characterization

Phase formation and the crystal structures of the synthesized powders and bulk  $\text{BaTiO}_3$  ceramics were performed using an X-ray diffractometer (XRD, Rigaku RINT 2000, Japan). A field emission scanning electron microscopy (FE-SEM, Hitachi S-4300, Japan) and a transmission electron microscopy (TEM, JEM-2010, JEOL, Japan) were used to observe the grain morphologies of the sintered samples and the sintering behaviors. The particle size distribution of the synthesized powders was measured by a laser particle analyzer (Horiba, LA-920, Japan). Ba/Ti ratio in the synthesized  $\text{BaTiO}_3$  powders was determined using inductively coupled plasma spectroscopy (ICP, IRIS Advantage, thermo Electron K.K., Japan) and energy dispersive spectroscopy (TEM-EDS, JEM-2010, JEOL, Japan). The average grain sizes of the bulk  $\text{BaTiO}_3$  ceramics were estimated from FE-SEM photographs. Sintering behavior was evaluated by measuring the relative densities of the sintered compacts. For sample characterization, five pellets were prepared. The dilatometric curves were recorded at a heating rate of  $100^\circ\text{C}/\text{h}$ , (TD-5200SA, Bruker-axs, Japan). The apparent linear shrinkage curves were corrected to obtain the evolution of the relative linear shrinkage.

## 3. Results and discussion

XRD investigations have shown that the powders synthesized by hydrothermal reaction with or without ball milling were crystallized as cubic- $\text{BaTiO}_3$  because the X-ray diffraction peak at  $2\theta \sim 45^\circ$  (i.e., (2 0 0) peak) is a single peak (Fig. 2a). These patterns revealed that  $\text{BaTiO}_3$  powders could be synthesized at  $100^\circ\text{C}$  by hydrothermal reaction. In addition, the Ba/Ti ratio of the synthesized powders with/without ball milling system was estimated to be 1.006 and 1.007 from inductively coupled plasma spectroscopy and energy dispersive spectroscopy, respectively. The XRD profiles of the (2 0 0), (2 1 0) and (2 1 1) peaks are given in Fig. 2b. The dotted lines represent the theoretical  $\text{BaTiO}_3$  peak

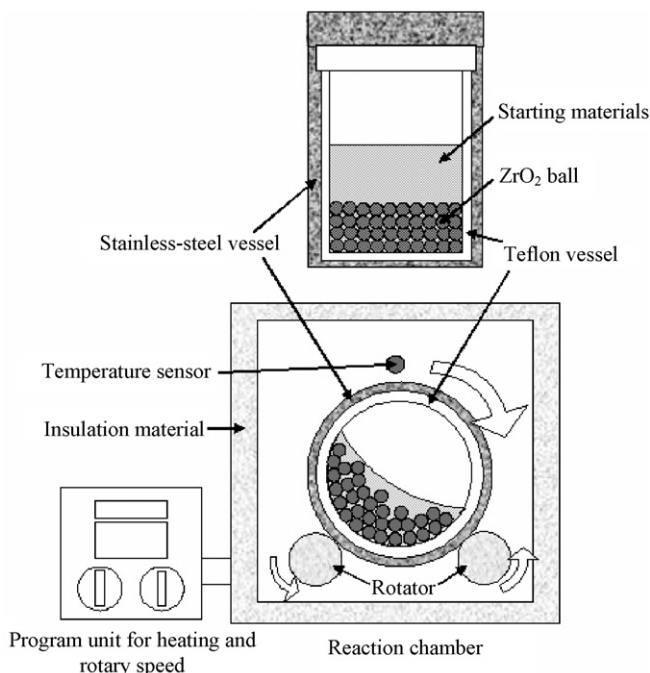


Fig. 1. Hydrothermal apparatus developed for this study.

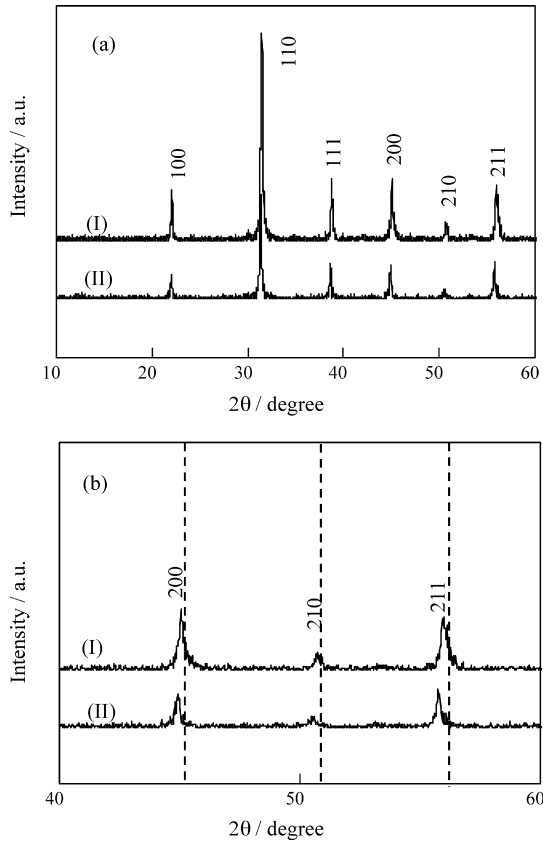


Fig. 2. (a) XRD patterns of the powders synthesized by a hydrothermal reaction without ball milling system (I)/with ball milling system (II) at 100 °C for 2 h. (b): XRD diffraction profiles of (2 0 0), (2 1 0) and (2 1 1) peaks.

positions of (2 0 0), (2 1 0) and (2 1 1). The peaks of hydrothermal powders are shifted to the lower angles as compared to the theoretical ones. Furthermore, the shift is much larger for the powder prepared from hydrothermal reaction assisted with ball milling. This shift can be attributed to the expansion and the strain of the lattice introduced by ball milling in the synthesized particles.<sup>18,19</sup> It is reported that the expanded unit cell of the syn-

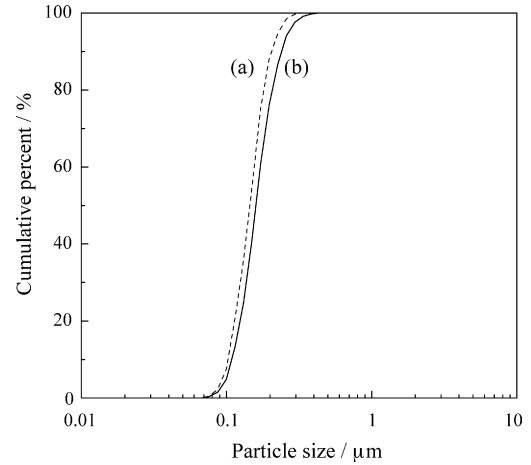


Fig. 4. Particle size distributions of the powders synthesized by (a) hydrothermal reaction with ball milling and (b) hydrothermal reaction without ball milling.

thesized BaTiO<sub>3</sub> powders results from water and hydroxyl ions (OH<sup>-</sup>) in the perovskite lattice after hydrothermal processing.<sup>18</sup>

Fig. 3 shows FE-SEM photographs of the synthesized powders obtained after a hydrothermal reaction with or without ball milling system operated at 100 °C for 2 h, and the fracture surfaces of bulk BaTiO<sub>3</sub> compacts sintered at 880, 900, 950 and 1000 °C for 5 h. Moreover, the relative densities of the sintered compacts are given for each one. The morphologies of the powders synthesized by ball-milling assisted hydrothermal reaction were similar to those prepared by hydrothermal synthesis without ball milling in that they are uniformly agglomerated to ~150 nm. The agglomerated particle size was in agreement with the results measured by particle size distribution analyzer (Fig. 4). The median particle size of the powders synthesized with/without ball milling was 140 and 150 nm, respectively. Moreover, the distribution was very narrow and unimodal. In addition, the primary particle size was estimated to be about 20 nm from the TEM observations. From these results, the morphology and the aggregation degree of the powders synthesized by hydrothermal reaction with/without ball

	Synthesized powders	880 °C	900 °C	950 °C	1000 °C
Without ball milling		R.D. 56.8% 	R.D. 60.0% 	R.D. 76.5% 	R.D. 94.3% 
With ball milling		R.D. 88.8% 	R.D. 96.5% 	R.D. 98.0% 	R.D. 98.6% 

Fig. 3. FE-SEM photographs of the synthesized powders obtained after a hydrothermal reaction with or without ball milling system operated at 100 °C for 2 h, and the fracture surfaces of the ceramics sintered at 880, 900, 950 and 1000 °C for 5 h.

milling seem similar. As shown in Fig. 3, the grain-size of the sintered compacts from hydrothermal reaction without ball milling was about 150 nm at 880 °C, which is similar to the starting particle size of the agglomerated powders. This indicates that sintering of each agglomerated particle is likely to occur at first. The relative density of the sintered compact was 56.8%. On the other hand, in the case of the sintered compacts produced by ball-milling assisted hydrothermal reaction, the sintering among the agglomerated powders has already started at 880 °C. The relative density of the sintered compact was 88.8%. Moreover, the microstructure of the sintered compacts, which were prepared by ball-milling assisted hydrothermal reaction, at 900 °C exhibited a rather homogeneous grain-size distribution with an estimated average grain size less than 1  $\mu\text{m}$ . The relative density of the compact prepared using ball-milling assisted hydrothermal reaction reached 96.5% in contrast to 60.0% for that prepared without ball milling. Hence, these results strongly suggest that dense BaTiO<sub>3</sub> ceramics can be fabricated at fairly low-sintering temperature (900 °C) using the powders produced by ball-milling assisted hydrothermal reaction. In general, it is known that the sintering temperature of BaTiO<sub>3</sub>, which is prepared from solid-state synthesis, is above 1300 °C. Densification to 96.5% at 900 °C, 98.0% at 950 °C, and 98.6% at 1000 °C clearly states that the green compacts of BaTiO<sub>3</sub> powders synthesized by ball-milling assisted hydrothermal reaction have a higher sinterability at lower temperatures.

Fig. 5 represents the XRD patterns ( $2\theta$  42–48°) of the BaTiO<sub>3</sub> compacts sintered at 900 and 1000 °C. The tetragonal structure is readily ascertained from the splitting of (200) peak around  $2\theta$  45°. Therefore, the crystalline phase of the sintered BaTiO<sub>3</sub> compacts is tetragonal. Note that crystalline structure of the synthesized powders was cubic as evidenced from Fig. 2.

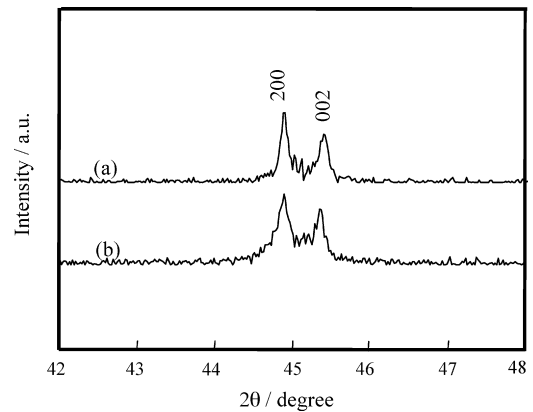


Fig. 5. XRD diffraction profiles of (200) and (002) for the BaTiO<sub>3</sub> ceramics sintered at (a) 1000 and (b) 900 °C for 5 h.

Fig. 6 shows TEM photographs of the sintered BaTiO<sub>3</sub> ceramics prepared from the powders synthesized after hydrothermal reaction with or without ball milling. It is seen that the ceramics have pores in the grain at lower sintering temperatures before significant densification took place. The pores are not observable with increasing densification. Grain growth is not caused by the solid-state reaction among particles during sintering, but is propelled by minimization of surface energy via surface and volume diffusion. Then, the pores decrease during the grain growth. From the TEM photographs of samples produced by hydrothermal reaction without ball milling (Fig. 6), it is observed that the mass is moved from the boundary at 950 and 1000 °C at which the grain growth occurred and that the pores in the grain are not seen. On the other hand, in the case of samples produced by ball-milling assisted hydrothermal reaction, the pores in the grain are not observed at lower-sintering temperature (900 °C), at which the grain growth occurred and the density of

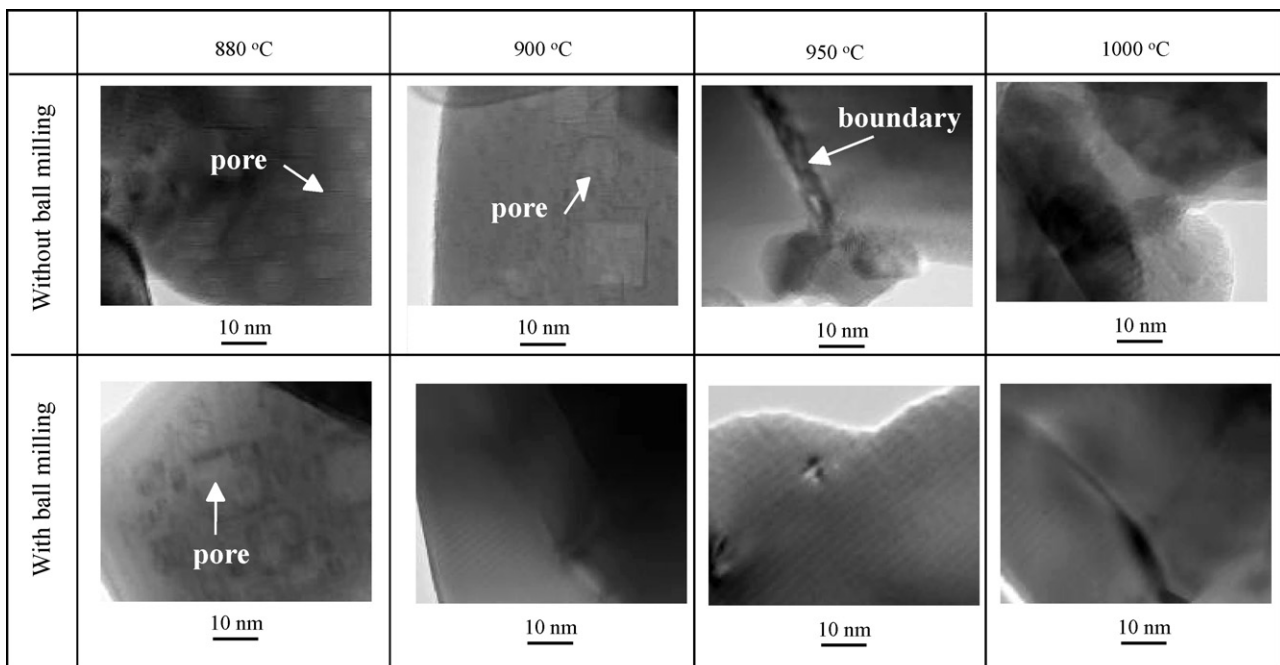


Fig. 6. TEM photographs of sintered BaTiO<sub>3</sub> ceramics prepared from the powders synthesized by hydrothermal reaction with or without ball milling.



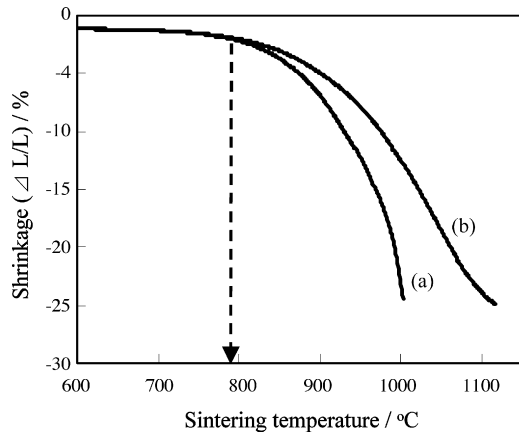


Fig. 7. Dilatometric curves for green compacts prepared from powders which are synthesized by hydrothermal reaction (a) with or (b) without ball milling.

sintered body became higher compared with samples prepared by hydrothermal reaction without ball milling. It is suggested that the mass transfer of the samples produced by ball-milling assisted hydrothermal reaction was occurred at low temperature and, thus, the sintering was promoted.

The dilatometric curves for green compacts from powders synthesized by hydrothermal reaction with or without ball milling are shown in Fig. 7. The curves show that shrinkage for both green compacts starts at 780 °C. However, as the sintering temperature increases, the sintering behavior changes in that the sintering rate of the sample prepared by hydrothermal reaction assisted with ball milling becomes faster than that prepared without ball milling. For example, the shrinkage is 8% at 900 °C and 24% at 1000 °C in the former as compared to 5% at 900 °C and 13% at 1000 °C in the latter. These results obviously show that ball milling during hydrothermal reaction gives rise to enhanced sinterability (or densification) at lower temperatures, as also shown in Fig. 3. Generally, it is known that hydroxyl ions ( $\text{OH}^-$ ) in perovskite lattice of hydrothermal  $\text{BaTiO}_3$  are almost removed at temperature  $\leq 800$  °C.<sup>20</sup> Therefore, the expanded unit fabricated by hydrothermal reaction does not cause acceleration of densification and grain growth because the densification (or shrinkage) starts at temperature  $>780$  °C (Fig. 7). The degree of powders aggregation (Figs. 3 and 4) and the relative density of green compacts were the similar as samples prepared from hydrothermal reaction without ball milling in those prepared from ball milling assisted hydrothermal reaction. In addition, mechanical force during the reaction leads to surface damage on each particle causing broken bonds. Therefore, it is thought that difference in surface energy between milled and not milled particles during synthesis influences sinterability at lower temperatures. The activation energy for sintering process can be readily determined from the sintering data.<sup>21</sup> Grain size

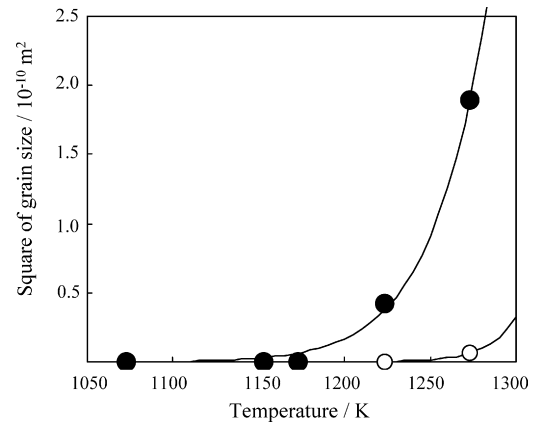


Fig. 8. Square of grain size as a function of sintering temperature. Filled circle: the compacts prepared by ball-milling assisted hydrothermal reaction. Open circle: the compacts prepared by hydrothermal reaction without ball milling.

is represented as:

$$G^2 - G_0^2 = Kt \quad (1)$$

where  $G$  is the grain size at sintering time  $t$  and  $G_0$  is the initial grain size. When  $t=0$  then,  $G = G_0$ . In general,  $G \gg G_0$  and then Eq. (1) becomes:

$$G^2 = Kt \quad (2)$$

In reaction kinetics,  $K$  is represented as follows;

$$K = \left( \frac{8x\gamma_b V_M}{N_A h} \right) \exp \left( \frac{-\Delta G^*}{RT} \right) \quad (3)$$

where  $N_A$  is Avogadro's number,  $h$  the Planck's constant,  $\gamma_b$  the surface energy,  $V_M$  the molar volume and  $x$  is the distance moved by an atom across the grain boundary. Substitution of Eq. (3) into Eq. (2) reveals the correlation between grain size and sintering temperature ( $T$ );

$$G^2 = \left( \frac{8x\gamma_b V_M}{N_A h} \right) t \exp \left( \frac{-\Delta G^*}{RT} \right) \quad (4)$$

where  $\Delta G^*$  is the activation energy for grain growth. Relationship between square of grain size and sintering temperature using the compacts of the synthesized  $\text{BaTiO}_3$  from hydrothermal reaction with or without ball milling is shown in Fig. 8. The graph was fitted to an equation,  $Y = a \exp(-b/X)$ . Table 1 shows the fitted equation and the activation energy for grain-growth ( $\Delta G^*$ ) in the present work. In the case of the sample prepared by ball-milling assisted hydrothermal reaction, the free energy for grain-growth activation was  $4.2 \times 10^5$  J/mol, whereas it was  $8.4 \times 10^5$  J/mol as for the sample produced by hydrothermal reaction without ball milling process. Hence, the activation energy for grain-growth decreases by half due to ball milling

Table 1  
Fitted equation and activation energy for grain growth ( $\Delta G^*$ ) estimated from Fig. 8

	Fitted equation	Activation energy for grain growth ( $\Delta G^*$ )
Without ball milling	$Y = 1.30 \times 10^{23} \exp(-1.01 \times 10^5/X)$	$8.4 \times 10^5$ J/mol
With ball milling	$Y = 4.08 \times 10^7 \exp(-5.08 \times 10^4/X)$	$4.2 \times 10^5$ J/mol

during hydrothermal reaction. As a result, the grain growth is promoted at lower sintering temperatures.

#### 4. Conclusions

BaTiO<sub>3</sub> powders were synthesized at 100 °C by hydrothermal reaction with and without ball milling. The powders synthesized by hydrothermal reaction with and without ball milling were uniformly agglomerated to ~150 nm, although the primary particle size was about 20 nm estimated from the TEM observations. BaTiO<sub>3</sub> powders synthesized by ball-milling assisted hydrothermal reaction were densified to 96.5% of theoretical density at a fairly low sintering temperature of 900 °C as compared to 60% of theoretical density in the ceramics prepared from powders synthesized by hydrothermal reaction without ball milling. The SEM, TEM observations and dilatometric curves showed the sintering rate of bulk BaTiO<sub>3</sub> ceramics prepared by ball-milling assisted hydrothermal reaction was faster. The activation energy for grain growth of the BaTiO<sub>3</sub> ceramics fabricated from powders synthesized by hydrothermal reaction with and without ball milling was calculated to be  $4.2 \times 10^5$  and  $8.4 \times 10^5$  J/mol, respectively. As a result, grain growth during sintering was promoted at lower temperature. Low temperature sintering of BaTiO<sub>3</sub> ceramics may be attributed to difference of surface energy induced by ball milling during the hydrothermal reaction. This new processing approach (e.g., ball-milling assisted hydrothermal reaction) enables us to fabricate dense BaTiO<sub>3</sub> ceramics at fairly low-sintering temperatures.

#### Acknowledgements

This work was supported by “Research and Development of the Low Environmental Burden Process” under the joint research with NGK INSULATORS, LTD.

#### References

- Song, Z. Q., Wang, S. B., Yang, W., Li, M., Wang, H. and Yan, H., Synthesis of manganese titanate MnTiO<sub>3</sub> powders by a sol–gel–hydrothermal method. *Mater. Sci. Eng. B*, 2004, **113**, 121–124.
- Bruno, S. A. and Swanson, D. K., High-performance multilayer capacitor dielectrics from chemically prepared powders. *J. Am. Ceram. Soc.*, 1993, **76**, 1233–1241.
- Yanez, C. G., Benitez, C. and Ramirez, H. B., Mechanical activation of the synthesis reaction of BaTiO<sub>3</sub> from a mixture of BaCO<sub>3</sub> and TiO<sub>2</sub> powders. *Ceram. Int.*, 2000, **26**, 271–277.
- Segal, D. L., Sol–gel processing: routes to oxide ceramics using colloidal dispersions of hydrous oxides and alkoxide intermediates. *J. Non-Cryst. Solids*, 1984, **63**, 183–190.
- Shimooka, H., Kohiki, S., Kobayashi, T. and Kuwabara, M., Preparation of translucent barium titanate ceramics from sol–gel derived transparent monolithic gels. *J. Mater. Chem.*, 2000, **10**, 1511–1522.
- Xia, C. T., Shi, E. W., Zhong, W. Z. and Guo, J. K., Preparation of BaTiO<sub>3</sub> by the hydrothermal method. *J. Eur. Ceram. Soc.*, 1995, **15**, 1171–1176.
- Xu, H. and Gao, L., Hydrothermal synthesis of high-purity BaTiO<sub>3</sub> powders: control of powder phase and size, sintering density, and dielectric properties. *Mater. Lett.*, 2004, **58**, 1582–1586.
- Pinceloup, P., Courtois, C., Leriche, A. and Thierry, B., Hydrothermal synthesis of nanometer-sized barium titanate powders: control of barium/titanium ratio, sintering, and dielectric properties. *J. Am. Ceram. Soc.*, 1999, **82**, 3049–3056.
- Xu, H. and Gao, L., Tetragonal nanocrystalline barium titanate powder: preparation, characterization, and dielectric properties. *J. Am. Ceram. Soc.*, 2003, **86**, 203–205.
- Lisoni, J. G., Lei, C. H., Hoffmann, T. and Fuenzalida, V. M., Hydrothermal growth of BaTiO<sub>3</sub> on TiO<sub>2</sub> single crystals. *Surf. Sci.*, 2002, **515**, 431–440.
- Pithan, C., Hennings, D. and Waser, R., Progress in the synthesis of nanocrystalline BaTiO<sub>3</sub> powders for MLCC. *Int. J. Appl. Ceram. Tech.*, 2005, **2**, 1–14.
- Kwon, S. W. and Yoon, D. H., Tetragonality of nano-sized barium titanate powder prepared with growth inhibitors upon heat treatment. *J. Eur. Ceram. Soc.*, 2007, **27**, 247–252.
- Moon, J., Suvaci, E., Morrone, A., Costantino, S. A. and Adair, J. H., Formation mechanisms and morphological changes during the hydrothermal synthesis of BaTiO<sub>3</sub> particles from a chemically modified, amorphous titanium (hydrous) oxide precursor. *J. Eur. Ceram. Soc.*, 2003, **23**, 2153–2161.
- Xu, H. and Gao, L., New evidence of a dissolution-precipitation mechanism in hydrothermal synthesis of barium titanate powders. *Mater. Lett.*, 2002, **57**, 490–494.
- Chaiyot, T., Acceleration of particle breakage rates in wet batch ball milling. *Powder Tech.*, 2002, **124**, 67–75.
- Lencka, M. M. and Riman, R. E., Thermodynamic modeling of hydrothermal synthesis of ceramic powders. *Chem. Mater.*, 1993, **5**, 61–70.
- Ahniyaz, A., Fujiwara, T., Song, S. W. and Yoshimura, M., Low temperature preparation of β-LiFe<sub>5</sub>O<sub>8</sub> fine particles by hydrothermal ball milling. *Solid State Ionics*, 2002, **151**, 419–423.
- Hennings, D. and Schreinemacher, S., Characterization of hydrothermal barium titanate. *J. Eur. Ceram. Soc.*, 1992, **9**, 41–46.
- Art, G., Hennings, D. and de With, G., Dielectric properties of fine-grained barium titanate ceramics. *J. Appl. Phys.*, 1985, **58**, 1619–1625.
- Wada, S., Tsurumi, T., Chikamori, H., Noma, T. and Suzuki, T., Preparation of nm-sized BaTiO<sub>3</sub> crystallites by a LTDS method using a highly concentrated aqueous solution. *J. Cryst. Growth*, 2001, **229**, 433–439.
- Hotta, Y., Microstructural changes in sintered Al<sub>2</sub>O<sub>3</sub> by acid treatment of compacts produced by slip casting in gypsum molds. *Ceram. Int.*, 2002, **28**, 593–599.